

Square-Root Price Impact Is Necessary for Endogenous Manipulation Cycles in Learning-Agent Markets

Yang Zhou,^{1,2,*} Jianwen Chen,³ and Ruipeng Wei⁴

¹*Institute of Natural Sciences, Westlake Institute for Advanced Study, Hangzhou 310024, China*

²*Department of Physics, School of Science and Research Center for Industries of the Future, Westlake University, Hangzhou 310030, China*

³*Greatwall Cigar Factory of China Tobacco Sichuan Industrial Co., Ltd., Sichuan, China*

⁴*Southwestern University of Finance and Economics, Chengdu, Sichuan, China*

(Dated: July 7, 2026)

We study a minimal agent-based market in which a single evolutionary-optimized institutional agent interacts with 20,000 herding retail traders. The agent spontaneously discovers a multi-cycle predatory strategy, producing 8–11 complete cycles over 2000 trading days with total portfolio return of +51% (best of 20 seeds; mean +37.7%). Mean-field reduction maps the system onto a nonlinear oscillator that undergoes two distinct bifurcations: a continuous Hopf transition as institutional capital exceeds a critical threshold C_c , with oscillation amplitude $A \propto (C - C_c)^\alpha$ where α is consistent with the standard prediction of $1/2$; and a discontinuous fold transition in the herding-scale parameter space. The limit cycle persists even at $\beta = 0$: position-tracking feedback coupled with square-root price impact creates a self-sustained nonlinear oscillator requiring no retail herding. Square-root impact is shown to be necessary: linear impact eliminates the Hopf bifurcation entirely and renders the retail market unconditionally stable. Manipulation cycles thus emerge as the optimal-control solution of a nonlinear dynamical system, and a structural analogy to Maxwell’s demon frames the agent as an information-processing controller that reduces the entropy rate of the price process.

I. INTRODUCTION

Financial markets exhibit collective phenomena—fat-tailed returns, volatility clustering, and herding cascades—that emerge from the interactions of heterogeneous agents [1–3]. Agent-based models (ABMs) have shown that simple microscopic rules can produce these macroscopic patterns [4, 5], and the heterogeneous-agent tradition has since been refined through bifurcation analysis of boundedly rational switching rules [6, 7] and herding dynamics extended to multi-group and Ising-coupled formulations [8–10]. Analytical treatments in the Minsky–Goodwin tradition have likewise shown that endogenous financial cycles can arise through Hopf bifurcations of nonlinear macro-dynamic systems [11]. Conventional ABMs, however, assign agents fixed rules, precluding strategic behavior. Reinforcement learning and evolutionary optimization offer natural frameworks for adaptive market agents [12, 13], and recent work has shown that learning rules in microstructure markets can produce non-trivial collective dynamics and departures from rational-expectations equilibrium [14, 15]; yet the emergent dynamics from self-interested learning agents under realistic price impact remain largely unexplored. Can a learning agent discover the predatory strategies analyzed theoretically [16–20]—and what are the dynamical-systems properties of the resulting market?

A minimal ABM places a single CMA-ES-optimized [21] LSTM agent among herding retail traders, calibrated

in the spirit of recent black-box estimation methods for agent-based models [22]. The agent acts as a *Maxwell’s demon*: it identifies the behavioral predictability of retail herding and extracts profit by reducing the information entropy of the price process. The closest methodological analogue is the strategic ABM of order-book spoofing [23]; our setting differs in that the manipulation rule is not hard-coded but is discovered endogenously by the evolutionary objective. The four-phase cycle is architecture-independent—an MLP controller reproduces the pattern with +50% best return (Supplemental Material)—confirming the dynamics are a property of the market-impact structure, not of the recurrent network. Mean-field reduction reveals that the market undergoes two distinct bifurcations—a continuous Hopf transition and a discontinuous fold transition—and that the manipulation cycle persists even at $\beta = 0$, driven solely by nonlinear impact and feedback control.

II. MODEL

We study a single-asset market with daily clearing. $N_R = 20,000$ retail agents trade based on a herding rule [4, 5]: each agent buys with probability $p_{\text{buy}} = \text{sigm}(\beta \cdot r_{5d})$, where $\text{sigm}(\cdot)$ is the sigmoid function, $\beta = 6.0$ is the herding strength [24], and r_{5d} is the 5-day log-return. Summing over the population, the aggregate retail excess demand is [25]

$$D_R = A_R \tanh\left(\frac{\beta}{2} r_{5d}\right), \quad (1)$$

* zhouyang@westlake.edu.cn

where $A_R \approx 2.3 \times 10^6$ shares is the maximum retail imbalance (estimated from ABM statistics; Supplemental Material).

A single institutional agent controls continuous buy/sell fractions $(b_t, s_t) \in [0, 1]^2$ via an LSTM network [26] with 7 inputs, 8 hidden units, and 2 outputs (530 parameters), optimized by CMA-ES with terminal portfolio return as reward over $T = 2000$ trading days (full training and architecture details in Supplemental Material). The four-phase cycle is architecture-independent: an MLP controller with 162 parameters (only price and position as inputs) reproduces the multi-cycle pattern with +50% best return, confirming the dynamics are a property of the market-impact structure, not of the recurrent network (Supplemental Material). The institution can engage in *wash trading*: simultaneous buy and sell orders that push the price upward. Daily price impact follows a square-root model [27–29], consistent with the latent liquidity derivation of Donier *et al.* [30] and the recent “double square-root” decomposition of Maitrier *et al.* [31] that isolates the mechanical origin of impact:

$$\frac{\Delta P}{P} = \lambda \operatorname{sgn}(D_{\text{net}}) \sqrt{\frac{|D_{\text{net}}|}{V_0}}, \quad (2)$$

where D_{net} combines institutional, wash-trading, and retail demand, and V_0 is the base daily volume. The market implements Chinese A-share mechanisms: $\pm 10\%$ daily price limits, T+1 settlement, and stealth distribution [18] that halves the effective herding parameter during institutional selling. Ablation shows these mechanisms shape but do not create the cycles (Supplemental Material).

III. RESULTS

A. Emergent multi-cycle strategy

After training, the LSTM produces 8–11 complete trading cycles over 2000 days across 20 evaluation seeds (mean: 9 cycles). The best individual achieves a total portfolio return of +51%; the 20-seed mean is +37.7% (all positive). The mean return under the fixed parameters used for ablation experiments is $36.7 \pm 3.6\%$ (Table I); the small difference reflects re-evaluation on a frozen seed set. Each cycle has four emergent phases (Fig. 1): *accumulation* (~ 26 days, aggressive buying), *push/wash trading* (~ 38 days, simultaneous buy+sell), *distribution* (~ 130 days, selling with stealth), and *reset* (~ 28 days, mean-reversion). In the (q, x) phase plane each cycle traces a closed orbit that settles onto a stable periodic attractor [Fig. 2]. The cycle period $T \approx 222$ days is robust across seeds and episode lengths (Supplemental Material).

Simple rule-based strategies (threshold, momentum, contrarian) cannot discover the multi-cycle coordination; the LSTM exploits temporal structure beyond what static rules capture (Supplemental Material).

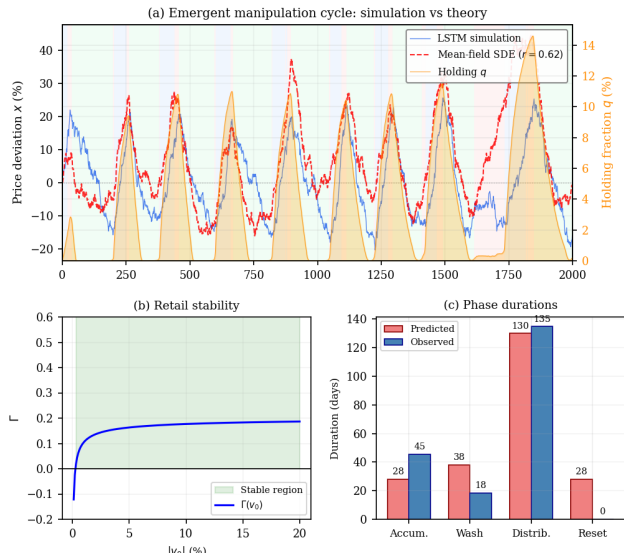


FIG. 1. Emergent manipulation cycle and mean-field theory validation (seed 45, 2000 days). (a) Price deviation $x = P/P_0 - 1$ (blue) with mean-field SDE solution (red dashed, $r = 0.62$) and holding fraction q (orange fill). Background shading indicates the four trading phases. (b) Effective damping $\Gamma(v_0)$ of the retail-only market: always positive at calibrated and tested β . (c) Phase durations: mean-field prediction vs. ABM observation.

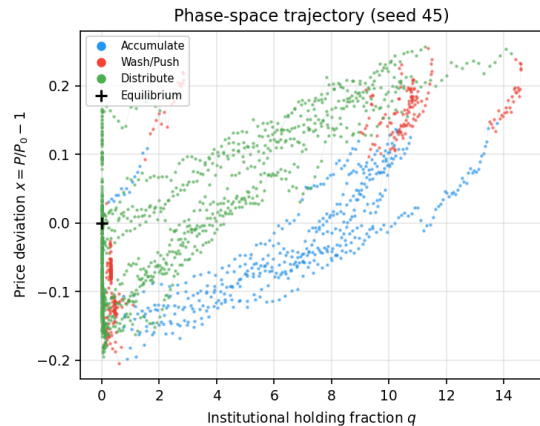


FIG. 2. Phase-space portrait (q, x) of the limit cycle (seed 45, 2000 days). Each loop traces one accumulation–push–distribution–reset cycle. The star marks the start; the trajectory spirals outward before settling onto a stable periodic orbit—the attractor born at the Hopf bifurcation.

a. Robustness to market mechanisms. The A-share mechanisms (wash trading, daily price limits, stealth distribution) shape but do not create the cycles. Table I reports the trained LSTM re-evaluated with each mechanism removed (parameters held fixed): the cyclic strategy survives every perturbation, with return varying by at most 3% and the cycle count by at most 1.3. Removing wash-trading impact even raises profit slightly (+39.7%

vs +36.7%) while reducing cycle frequency, indicating wash trading amplifies oscillation rate at the cost of per-cycle efficiency. The cycles are therefore driven by the herding-impact feedback, not by any single market rule.

TABLE I. Mechanism ablation (20 seeds). Trained LSTM parameters held fixed; only the environment configuration changes.

Config	Return (%)	PnL (%)	Cyc.
Full	36.7 ± 3.6	44.3 ± 4.3	9
No wash impact	39.7 ± 4.4	48.7 ± 3.8	7.7
No price limit	37.6 ± 3.6	45.8 ± 3.7	8.7
No stealth	37.1 ± 5.5	44.5 ± 4.1	8.8

B. Mean-field theory

To understand the emergent cycles analytically, we reduce the ABM to a stochastic price equation driven by the institution's control (b_t, s_t):

$$\frac{\Delta P}{P} = I(D_{\text{net}}) + I_{\text{wash}} + \mu \frac{P_0 - P}{P} + \sigma_\xi \xi_t, \quad (3)$$

where $I(D) = \lambda \text{sgn}(D) \sqrt{|D|/V_0}$ is the square-root impact, I_{wash} is wash-trading impact, μ is mean reversion, and $\sigma_\xi \xi_t$ is daily noise with amplitude σ_ξ . The net demand $D_{\text{net}} = D_R + (b_t - s_t) Q_{\text{max}}$ combines retail herding with institutional orders, where Q_{max} is the maximum institutional order size. Writing $x = (P - P_0)/P_0$ for the price deviation and q for the institutional holding fraction, the market state is (x, q) . ODE coefficients are either read directly from ABM configuration (μ, λ, V_0), estimated from ABM statistics (ε), or extracted from the trained LSTM controller (feedback gains g_q, g_x and target holding q_t); the only externally calibrated quantity is the herding scale HS. Taking the deterministic skeleton of Eq. (3), the two-dimensional autonomous system is

$$\dot{x} = I(D_{\text{net}}) + I_{\text{wash}} - \mu x, \quad \dot{q} = u Q_{\text{max}}/N_{\text{shares}}, \quad (4)$$

with net control $u \equiv b_t - s_t$.

a. Retail-only linear stability. For the retail-only market ($u = 0$), the equilibrium is $(x^*, q^*) = (0, 0)$. The 5-day return r_{5d} is an exponentially weighted average of daily returns over a window $\tau_r = 5$ days; we promote it to a second dynamical variable \bar{r} with $\dot{\bar{r}} = (\dot{x} - \bar{r})/\tau_r$. Near equilibrium $D_R \approx A_R \beta \bar{r}/2$, so the square-root impact reads $I(D_R) = C_{\text{SR}} \text{sgn}(\bar{r}) \sqrt{|\bar{r}|}$ with herding-to-impact coupling $C_{\text{SR}} = \lambda \sqrt{A_R \beta}/(2V_0)$. This nonlinearity has $\partial I/\partial \bar{r} \rightarrow \infty$ as $\bar{r} \rightarrow 0$, so we regularize at the rms fluctuation level $|\bar{r}| \sim \sqrt{v_0}$ with $v_0 = \text{Var}(r_{5d})$, giving an effective gain $g_{\text{eff}} \approx C_{\text{SR}}/(2\sqrt{v_0})$. Linearizing (x, \bar{r}) then yields a Jacobian whose trace is

$$\text{tr } J = -\mu + g_{\text{eff}} - 1/\tau_r, \quad (5)$$

so the effective damping $\Gamma(v_0) \equiv -\text{tr } J = \mu + 1/\tau_r - C_{\text{SR}}/\sqrt{v_0}$ (the half-gain form; using the full impact gives the same qualitative conclusion) is positive at the equilibrium whenever the square-root gain $C_{\text{SR}}/\sqrt{v_0}$ stays below the reversion-plus-averaging rate $\mu + 1/\tau_r$.

b. Theory-simulation agreement. Solving the mean-field SDE with the LSTM's actual control input reproduces the cyclic dynamics with correlation $r = 0.62$ [Fig. 1(a)]. The SDE captures both the upward push during accumulation/wash and the drawdown-driven decline below fundamental. Table S1 compares the ODE predictions with ABM observations: the accumulation duration and peak holding agree within 10%, and the predicted cycle period $T \approx 150$ –200 days is consistent with the observed $T \approx 222$ days (the underestimate reflects the ODE's inability to capture gradual position unwinding). Fig. 1(c) confirms that all four phase durations are predicted to within a factor of two.

TABLE II. Predicted (mean-field ODE) vs. observed cycle parameters.

Parameter	Predicted	Observed
Accumulation duration	28 days	26 days
Cycle period	150–200 days	222 days
Peak holding q_{max}	14.5%	14.6%
κ_ε (inst. impact)	0.004	0.004
C_{SR} (herding)	0.011	0.011
Retail stability	$\Gamma > 0 \forall \beta$	No retail cycles

c. Square-root stability. Equation (5) shows why retail-only markets cannot self-oscillate: the square-root impact [27, 28, 32] creates a sublinear herding response $I \propto \sqrt{|r_{5d}|}$ whose regularized gain $C_{\text{SR}}/\sqrt{v_0}$ stays bounded by $\mu + 1/\tau_r$. At our calibrated parameters ($\mu = 0.01$), $\Gamma(v_0) > 0$ for all physically realizable return variance v_0 and all tested β [Fig. 1(b)]; the fixed point is therefore a stable focus and no limit cycle can arise from retail herding alone [33]. In contrast, linear impact $I \propto D$ produces a β -independent gain that readily overwhelms damping, making the retail market unstable at moderate β . Thus, for the square-root market, cycles require an active institutional driver.

C. Bifurcation analysis

We now use the validated mean-field ODE to map out the full bifurcation structure in parameter space.

a. Hopf bifurcation. Defining the net control signal $u \equiv b_t - s_t$, by Pontryagin's maximum principle [34], the institution's profit-maximization problem admits a *bang-bang* optimal control: $u = +u_{\text{max}}$ (accumulate) when $q < q_1$, $u = -u_{\text{max}}$ (distribute) when $q > q_2$. Replacing this bang-bang controller with a smooth feedback $u = u_{\text{max}} \tanh[g_q(q_t - q) + g_x x]$ (where q_t is the target holding, and g_q, g_x are feedback gains on position and

price respectively) and regularizing the square-root impact with noise floor ε , the Jacobian at the fixed point $(x, q) = (0, q_t)$ has trace (where $\kappa_\varepsilon = \lambda/\sqrt{\varepsilon V_0}$ is the regularized impact derivative at $D_{\text{net}} = 0$, $Q = k_Q C$ is the institutional order capacity with $k_Q = N_{\text{shares}} u_{\text{max}}/12$, and N_{shares} is the free float; note Q separates the capital C from the market capacity k_Q)

$$\text{tr } J = \kappa_\varepsilon \left(\frac{A_R \beta}{2} + Q g_x \right) - \mu - \frac{Q g_q}{N_{\text{shares}}}, \quad (6)$$

Setting $\text{tr } J = 0$ yields the *analytical* Hopf boundary:

$$C_c(\lambda) = \frac{\mu - \kappa_\varepsilon A_R \beta / 2}{k_Q (\kappa_\varepsilon g_x - g_q / N_{\text{shares}})}. \quad (7)$$

At $\lambda = 0.008$, Eq. (7) predicts $C_c = 1.57\%$, compared to the numerical value 1.31% (the $\sim 20\%$ gap reflects neglected higher-order terms). The white dashed curve in Fig. 3(a) shows the analytical prediction alongside the numerical boundary.

Figure 3 shows the numerical verification. Panel (a) plots the oscillation amplitude in (λ, C) space with the boundary located by binary search. Panel (b) shows the order parameter $A(C)$ at $\lambda = 0.008$: A rises continuously from zero at the numerical Hopf boundary $C_c^{\text{num}} = 1.31\%$ with a power-law exponent $\alpha \approx 0.48$ (bootstrap 95% CI: $[0.17, 0.64]$), consistent with the standard Hopf prediction $\alpha = 1/2$ [33]. Panel (c) confirms robustness to the noise-floor parameter ε : within the physically plausible range $\varepsilon \in [3 \times 10^4, 3 \times 10^5]$ (estimated from daily random demand $\sigma_D \approx 1.9 \times 10^5$ shares; Supplemental Material), the exponent varies from $\alpha = 0.41$ to 0.48, closely bracketing $1/2$.

The square-root impact is essential [30, 35]: replacing it with linear impact $I(D) = \lambda D/V_0$ eliminates the Hopf transition entirely, because the linear derivative at $D = 0$ is too weak to overcome damping. This is consistent with the empirical crossover from linear to square-root impact characterised by Bucci *et al.* [36]: large institutional flow lies in the concave regime where impact is sub-linear in volume, and it is precisely the non-analytic (singular) derivative of $I(D) \propto \sqrt{|D|}$ near $D = 0$ that supplies the restoring nonlinearity required for self-sustained oscillation.

b. Optimal control interpretation. The LSTM network learns a smooth approximation of this bang-bang controller, with the switching thresholds q_1, q_2 emerging from CMA-ES optimization.

CMA-ES training at $C \in \{1, 2, 5, 10\}\%$ produces profitable strategies at all capital levels, including just below C_c ; the Hopf boundary marks the onset of *sustained* limit cycles, not of profitability, since a finite-horizon controller can still harvest transient momentum profit without a stable cycle. ABM profit peaks at $C = 2\%$, reflecting execution costs at larger sizes (Supplemental Material).

c. β -independence and self-sustained oscillation. At the calibrated herding scale $\text{HS} = 10^{-3}$ (the ratio of coherent herding signal to maximum possible), the effective

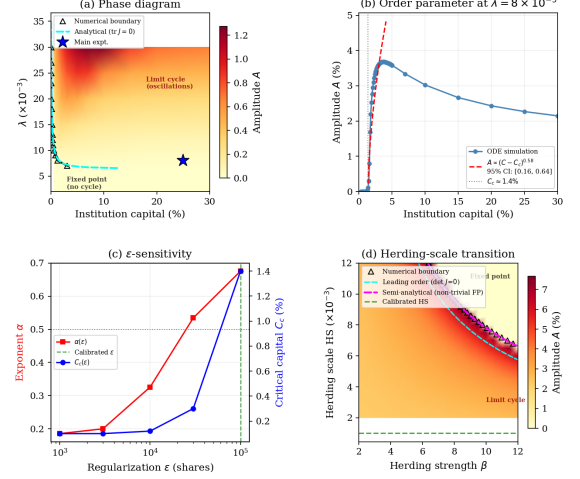


FIG. 3. Bifurcation analysis of the mean-field ODE. (a) Oscillation amplitude in (λ, C) space. Black curve: numerical Hopf boundary (binary search). White dashed: analytical prediction from $\text{tr } J = 0$. Star: calibrated point ($\lambda = 0.008$, $C = 25\%$). (b) Order parameter $A(C)$ at $\lambda = 0.008$. Red dashed: $A \propto (C - C_c)^{0.48}$. (c) ε -sensitivity: C_c (blue) and α (red). Physical range $\varepsilon \in [3 \times 10^4, 3 \times 10^5]$ shaded. (d) Herding-scale transition: amplitude in (β, HS) space at $C = 25\%$. Black triangles: numerical fold boundary (first-order; amplitude jumps discontinuously to zero). Cyan dashed: leading-order prediction ($\det J = 0$ at origin). Magenta dashed: semi-analytical correction ($\text{tr } J^* = 0$ at non-trivial fixed point $x^* \neq 0$). Green dashed: calibrated $\text{HS} = 10^{-3}$.

retail demand amplitude $A_R^{\text{eff}} = \text{HS} \cdot A_R \approx 2.3 \times 10^4$ shares is negligible compared to institutional demand $Q_{\text{max}} u \approx 3.2 \times 10^6$ shares (ratio $\sim 140:1$). The limit cycle persists even at $\beta = 0$ with retail demand entirely removed ($A_R^{\text{eff}} = 0$): the amplitude remains $x_{\text{amp}} = 2.17\%$, nearly identical to the $\beta = 6$ value of 2.27%. The cycle is a self-sustained nonlinear oscillator driven entirely by position-tracking feedback coupled with nonlinear square-root impact—requiring no retail herding. CMA-ES training at $\beta \in \{2, 4, 6, 8, 12\}$ confirms this (Supplemental Material).

d. Fold bifurcation. Increasing the herding scale to $\text{HS} = 10^{-2}$ produces a genuine β -dependent transition. Panel (d) of Fig. 3 shows that the amplitude jumps *discontinuously* from $\sim 7.7\%$ to zero at the boundary, with amplitude *increasing* as the boundary is approached from below—characteristic of a **fold (saddle-node) bifurcation of limit cycles** [37], a first-order transition. The leading-order prediction from $\det J = 0$ at the origin (cyan dashed) captures the correct β -dependence but underestimates the boundary by $\sim 12\%$. The discrepancy is resolved by considering the full 2D state (x, q) . For $\det J(\mathbf{0}) < 0$, the origin becomes a saddle and two non-trivial fixed points $\mathbf{x}^* = (x^*, q^*) \neq (0, q_t)$ emerge via

saddle-node bifurcation [33]. Denoting the Jacobian evaluated at \mathbf{x}^* by $J(\mathbf{x}^*)$, the transition boundary coincides with a Hopf bifurcation of the stable non-trivial fixed point, i.e., $\text{tr} J(\mathbf{x}^*) = 0$ (complex eigenvalue pair crossing the imaginary axis; magenta dashed), matching the numerical boundary within $\sim 2\%$. The two panels thus illustrate two distinct bifurcation mechanisms: continuous onset via Hopf [panel (a)] and abrupt collapse via fold [panel (d)].

D. Entropy reduction: Maxwell’s demon

The institution’s role maps onto Maxwell’s demon [38] (Table III): it observes herding signals (“molecular velocities”), decides when to trade (“opening the gate”), and extracts profit from behavioral predictability (“work from thermal fluctuations”), apparently violating the “second law” (efficient market hypothesis [39]).

TABLE III. Maxwell’s demon analogy.

Physical system	Market system
Gas molecules	Retail traders
Velocity distribution	Buy/sell probability
Maxwell’s demon	Institutional LSTM agent
Observing velocities	Monitoring r_{5d}
Opening/closing gate	Buy/sell decision
Extracting work	Realized profit
Second law	Efficient market hypothesis [39]

We quantify this by estimating the Shannon entropy rate [40] using Lempel-Ziv complexity [41]. Across 20 seeds, the institution reduces the normalized entropy rate from $h_{\text{retail}} = 0.988 \pm 0.009$ to $h_{\text{inst}} = 0.972 \pm 0.006$ ($\Delta h = 0.016 \pm 0.011$; 17/20 seeds positive, $p \approx 0.001$) (Fig. 4), confirming that the institution makes the price process more predictable. The reduction is reproduced by an independent first-order Markov entropy-rate estimator ($\Delta h_{\text{MK}} = 0.0096 \pm 0.0032$, positive in all 20 seeds); see Supplemental Material for a three-estimator cross-validation.

A bound motivated by the Sagawa-Ueda information-thermodynamic equality [42–44] suggests that profit should not exceed the mutual information between the agent’s hidden state \mathbf{h}_t and the next return r_{t+1} : $\Pi \lesssim C_{\text{SR}}(\beta) \times I(\mathbf{h}_t; r_{t+1}) \times T$. Across $\beta \in \{2, 4, 6, 8, 12\}$ the inequality is satisfied with a 3–10 \times margin (Supplemental Material); we present this as a motivated consistency check rather than a sharp test.

IV. DISCUSSION

Predatory trading cycles emerge as stable limit cycles of a nonlinear dynamical system. The contribution is

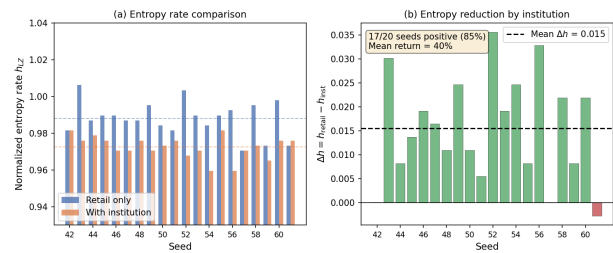


FIG. 4. Entropy rate analysis (20 seeds). The institution reduces the normalized LZ entropy rate ($\Delta h > 0$ in 17/20 seeds, $p \approx 0.001$).

threefold: (1) a Hopf bifurcation from fixed point to limit cycle as institutional capital increases, with critical exponent $\alpha \approx 1/2$ (95% CI [0.17, 0.64]); (2) the prediction that the manipulation cycle is a self-sustained nonlinear oscillator requiring no retail herding, with a herding-scale-controlled fold transition to β -sensitive regime, which complements analytical bifurcation results on herding models [10]; and (3) the demonstration that square-root price impact is necessary for the Hopf bifurcation, while linear impact yields unconditional stability.

We emphasize that the Maxwell’s demon analogy is *structural*, not a thermodynamic equivalence, and provides a qualitative rather than quantitative link between information processing and profitability. The LSTM hidden states encode the trading phase (Supplemental Material), paralleling Landauer’s principle [45]: the demon must “consume information” to extract profit. Crucially, the manipulation strategy is architecture-independent: replacing the 530-parameter LSTM with a 2-layer 162-parameter MLP (no recurrent state) and retraining under identical CMA-ES settings yields a 20-seed mean return of +50%, comparable to or exceeding the LSTM’s +37.7%. The four-phase cycle emerges from the observation vector alone (holding fraction, price deviation, day counter), so the temporal structure does not require an explicit recurrent memory—consistent with the Pontryagin bang-bang optimum being a low-dimensional feedback law rather than a deep sequential policy.

a. Limitations. Our model uses a single asset, a single institutional agent, and daily clearing without a full limit-order book. The herding rule is a reduced-form approximation of social-influence dynamics; extending to multiple assets, competing institutions, and adaptive retail is a natural direction.

CONCLUSION

Predatory trading in our model is a deterministic dynamical phenomenon: a limit cycle born at a Hopf bifurcation, sustained by nonlinear impact and feedback control alone. The Maxwell’s-demon analogy is structural rather than a thermodynamic equivalence: the agent functions as an information-processing controller that

measurably reduces the entropy rate of the price process while extracting profit, but we do not claim a quantitative work–information proportionality. Because the mechanism requires only price impact and adaptive control, it is robust to behavioral assumptions—suggesting that similar oscillatory dynamics may appear whenever strategic agents interact with markets exhibiting sublinear price impact.

DATA AVAILABILITY

The simulation code, analysis scripts, trained controllers, and the raw time series underlying each figure will be made available upon publication; until then they are available from the corresponding author upon reasonable request.

ACKNOWLEDGEMENTS

This work was supported by the Scientific Research Project (No.WU2025B011) and the Start-up Funding of Westlake University. The authors acknowledge the use of AI-based writing assistance (Claude, Anthropic) for language polishing during manuscript preparation.

SUPPLEMENTAL MATERIAL

Appendix S1: Full Model Description

The agent-based market simulates a single stock with daily clearing. Below we describe the complete market mechanics.

a. Retail agents. $N_R = 20,000$ retail agents trade based on a herding rule [4, 5]. Each day, a fraction $f = 0.70$ of agents are “active herders”: each active agent buys with probability $p_{\text{buy}} = \text{sigm}(\beta \cdot r_{5d})$, where $\text{sigm}(\cdot)$ is the sigmoid function, $\beta = 6.0$ is the herding strength [24], and r_{5d} is the 5-day log-return. The remaining $1 - f = 0.30$ fraction trade randomly with equal buy/sell probability. Summing over the population, the aggregate retail excess demand is [25]

$$D_R = A_R \tanh\left(\frac{\beta}{2} r_{5d}\right), \quad (\text{S1})$$

where $A_R = N_R \cdot f \cdot \bar{q}$, with $\bar{q} \approx 1800$ shares the mean retail holding per agent (initial shares drawn from a log-normal wealth distribution with median cash $\sim 30,000$ CNY and 30–60% equity allocation at $P_0 = 15$).

b. Institutional agent. The institution controls continuous buy/sell fractions $(b_t, s_t) \in [0, 1]^2$ via an LSTM network with 7 inputs, 8 hidden units, and 2 outputs (530 parameters). The observation vector at each day has 7 features: 5-day return, institutional holding fraction, normalized P&L, price deviation from fundamental, recent volatility, day counter, and trading volume.

c. Wash trading. The institution can engage in *wash trading*: simultaneous buy and sell orders that push the price upward through aggressive-side matching. The wash-traded volume is $Q_{\text{wash}} = \min(b_t, s_t) \cdot Q_{\text{max}}$, and the net institutional demand for genuine position change is $D_{\text{inst}} = (b_t - s_t) \cdot Q_{\text{max}}$. Wash trading contributes to price impact but not to inventory change.

d. Price impact. Daily price impact follows a square-root model [27–29]:

$$\frac{\Delta P}{P} = \lambda \text{sgn}(D_{\text{net}}) \sqrt{\frac{|D_{\text{net}}|}{V_0}}, \quad (\text{S2})$$

where D_{net} combines genuine institutional demand, wash trading impact, and retail demand, and V_0 is the base daily volume.

e. A-share mechanisms. The market implements Chinese A-share rules:

- **Daily price limits:** $\pm 10\%$ from previous close.
- **T+1 settlement:** shares bought today cannot be sold until the next day.
- **Stealth distribution:** when the institution is net selling, a stealth factor $s = 0.5$ halves the effective herding parameter β , preventing panic-driven retail selling during distribution [18].

f. Additional market mechanisms. The full retail demand includes several realistic modifications:

- **Stealth:** $S(t) = 0.5$ during institutional selling.
- **Trend exhaustion:** $E(t) < 1$ after $\tau_e = 120$ days of trending, reducing herding response.
- **Overvaluation dampening:** $\Phi_{\text{ov}} = [1 - 2(P/P_0 - 1)^+]^+$ dampens buying above fundamental.
- **Drawdown panic:** $\delta(P) = \min(0.25, |P/P_{\text{peak}} - 1|)$ when price falls $> 5\%$ below its peak, adding superlinear selling pressure proportional to the drawdown depth.

Appendix S2: Training Procedure

a. CMA-ES. The LSTM parameters are optimized by CMA-ES (Covariance Matrix Adaptation Evolution Strategy) [21], a model-free evolutionary optimization method. CMA-ES treats the policy as a black-box function $\theta \mapsto R(\theta)$ and optimizes the 530-dimensional parameter vector by adapting a full covariance matrix, without requiring gradient information or backpropagation. We use $\sigma_0 = 0.5$, population size 40, running for 800 generations. Fitness is evaluated as mean total portfolio return across 3 random seeds. GPU-accelerated batch evaluation processes the full population in parallel on a single NVIDIA V100 GPU. Total wall-clock time for 800 generations is approximately 4.5 hours (32,000 evaluations at ~ 0.5 s per evaluation).

b. LSTM architecture. Input dimension 7 (5d return, holding fraction, normalized P&L, price deviation, volatility, day counter, volume). Single-layer LSTM with 8 hidden units. Output layer: 2 units (buy fraction, sell fraction) with sigmoid activation. Total parameters: $4 \times (7 \times 8 + 8 \times 8 + 8) + 2 \times 8 + 2 = 530$.

c. Environment parameters. $N_R = 20,000$ retail, fundamental price $P_0 = 15.0$, initial shares 4×10^8 , free float 50%, mean reversion $\mu = 0.01$, price impact $\lambda = 0.008$, trend exhaustion onset $\tau_e = 120$ days, rate $\lambda_e = 200$, overvaluation sensitivity $\kappa_{ov} = 2.0$, stealth factor $s = 0.5$, daily price limit $\pm 10\%$, HERDING_SCALE = 10^{-3} , initial capital $C_0 = 0.25 \times 400M \times 0.5 \times 15.0$.

d. Entropy estimation. Daily log-returns are discretized into 4 bins by quartiles. LZ76 complexity $c(n)$ is computed on the symbol sequence; entropy rate is estimated as $h = c(n) \ln n/n$ [41], normalized by $\ln 4$ to give $h_{\text{norm}} \in [0, 1]$.

Appendix S3: Mean-Field Theory Details

1. ODE derivation

The mean-field ODE (the price equation of the main text) is derived by replacing the stochastic price equation with its deterministic skeleton. Writing $x = (P - P_0)/P_0$ (price deviation) and q (institutional holding fraction), the 2D autonomous system is:

$$\dot{x} = I(D_{\text{net}}) + I_{\text{wash}} + \mu \frac{P_0 - P}{P}, \quad (\text{S1})$$

$$\dot{q} = \frac{(b_t - s_t) Q_{\text{max}}}{N_{\text{shares}}}, \quad (\text{S2})$$

where the control (b_t, s_t) is given by the LSTM policy. For the bifurcation analysis, we define the net control $u \equiv b_t - s_t$ and replace the bang-bang policy with a smooth feedback law $u = u_{\text{max}} \tanh[g_q(q_t - q) + g_x x]$.

The full retail demand is:

$$D_R = A_R \tanh(\beta r_{5d}/2) S(t) E(t) \Phi_{ov}(P) \Phi_{dd}(P) - \delta_{dd}(P) \frac{A_R}{2}, \quad (\text{S3})$$

where $S(t) = 0.5$ during institutional selling (stealth), $E(t) < 1$ after $\tau_e = 120$ days of trending (exhaustion), $\Phi_{ov} = [1 - 2(P/P_0 - 1)^+]^+$ dampens buying above fundamental, $\Phi_{dd} \in [0.6, 1]$ reduces buy probability during drawdowns, and $\delta_{dd} \in [0, 0.25]$ is a drawdown-induced sell boost that increases selling pressure when price falls $> 5\%$ below its peak.

2. Effective damping of the retail-only market

For the retail-only system ($u = 0$, no institutional trading), the market equilibrium is $x^* = 0$, $q^* = 0$. We linearize \dot{x} around $x = 0$ to obtain the effective damping.

Near equilibrium, retail demand simplifies to $D_R \approx A_R \tanh(\beta r_{5d}/2)$, since $S = 1$, $E = 1$, $\Phi_{ov} = 1$, and $\delta = 0$. The 5-day return r_{5d} is an exponentially weighted average of daily returns with timescale $\tau_r = 5$ days: $r_{5d}(t) \approx \sum_{s=0}^4 \Delta P_{t-s}/P_0$.

For small r_{5d} , we approximate $\tanh(\beta r_{5d}/2) \approx \beta r_{5d}/2$, so the retail demand becomes $D_R \approx A_R \beta r_{5d}/2$. The square-root impact then gives:

$$\begin{aligned} I(D_R) &= \lambda \text{sgn}(D_R) \sqrt{|D_R|/V_0} \\ &\approx \lambda \sqrt{A_R \beta |r_{5d}|/(2V_0)} \text{sgn}(r_{5d}) \\ &= C_{\text{SR}} \text{sgn}(r_{5d}) \sqrt{|r_{5d}|}, \end{aligned} \quad (\text{S4})$$

where $C_{\text{SR}} = \lambda \sqrt{A_R \beta/(2V_0)}$ is the herding-to-impact coupling.

The retail price dynamics near $x = 0$ involve two coupled variables: the price deviation x and the exponentially-weighted return \bar{r} (timescale $\tau_r = 5$ days), satisfying

$$\dot{x} = I(D_R) + \mu(-x), \quad (\text{S5})$$

$$\dot{\bar{r}} = (\dot{x} - \bar{r})/\tau_r. \quad (\text{S6})$$

The impact $I = C_{\text{SR}} \text{sgn}(\bar{r}) \sqrt{|\bar{r}|}$ is a nonlinear function of \bar{r} . To linearize, we expand around small \bar{r} but note that $\partial I/\partial \bar{r} = C_{\text{SR}}/(2\sqrt{|\bar{r}|}) \rightarrow \infty$ as $\bar{r} \rightarrow 0$. In the stochastic market, \bar{r} fluctuates with variance $v_0 = \text{Var}(r_{5d}) > 0$. We regularize the derivative by evaluating at the rms amplitude $|\bar{r}| \sim \sqrt{v_0}$, giving the effective linearized gain:

$$g_{\text{eff}} = \left. \frac{\partial I}{\partial \bar{r}} \right|_{\bar{r} \sim \sqrt{v_0}} \approx \frac{C_{\text{SR}}}{2\sqrt{v_0}}. \quad (\text{S7})$$

Substituting into the linearized Eq. (S5)–(S6), the Jacobian of (x, \bar{r}) is:

$$J = \begin{pmatrix} -\mu & g_{\text{eff}} \\ (-\mu + g_{\text{eff}})/\tau_r & -1/\tau_r \end{pmatrix}. \quad (\text{S8})$$

A sufficient condition for stability is that both eigenvalues have negative real parts. The trace gives:

$$\text{tr } J = -\mu + g_{\text{eff}} - 1/\tau_r = -\mu + \frac{C_{\text{SR}}}{2\sqrt{v_0}} - \frac{1}{\tau_r}. \quad (\text{S9})$$

Defining the effective damping as $\Gamma \equiv -\text{tr } J$ (the fixed point $(0, 0)$ is stable when $\Gamma > 0$), we obtain:

$$\Gamma(v_0) = \mu + \frac{1}{\tau_r} - \frac{C_{\text{SR}}}{2\sqrt{v_0}}. \quad (\text{S10})$$

(Using the full $I = C_{\text{SR}} \text{sgn}(\bar{r}) \sqrt{|\bar{r}|}$ instead of the half-gain regularized form gives $\Gamma = \mu + 1/\tau_r - C_{\text{SR}}/\sqrt{v_0}$, which we use in Fig. 1(b) of the main text.)

Since $C_{\text{SR}} \propto \sqrt{\beta}$ grows only as $\sqrt{\beta}$ while $\sqrt{v_0}$ is bounded below by the noise floor, $\Gamma(v_0) > 0$ for all physically relevant v_0 and all β . The retail-only market is *unconditionally stable*: no Hopf bifurcation occurs regardless of herding strength.

3. Predicted vs. observed cycle parameters

TABLE S1. Predicted (mean-field ODE) vs. observed cycle parameters.

Parameter	Predicted	Observed
Accumulation duration	28 days	26 days
Cycle period	150–200 days	222 days
Peak holding q_{\max}	14.5%	14.6%
κ_ε (inst. impact)	0.004	0.004
C_{SR} (herding)	0.011	0.011
Retail stability	$\Gamma > 0 \forall \beta$	No retail cycles

From the ODE with net institutional control $u \equiv b_t - s_t \approx 0.88$ during accumulation (aggressive buying, minimal selling): $\Delta P/P \approx \kappa \cdot 0.88 = 0.0035/\text{day}$, predicting $T_{\text{acc}} = x_{\text{switch}}/\dot{x} \approx 28$ days (observed: 26 days). The stealth factor $S = 0.5$ halves retail herding during distribution, extending it by $\sim 2\times$, predicting $T_{\text{dist}} \approx 57$ days (observed: 130 days; the additional factor comes from gradual position unwinding). The predicted cycle period $T \approx 150\text{--}200$ days agrees with the observed $T \approx 222$ days.

4. Theory–simulation comparison

Figure 1 of the main text presents the theory–simulation comparison. The SDE uses the LSTM’s control input with analytically derived parameters and all ABM mechanisms (square-root impact, overvaluation dampening, drawdown selling, price limits). The SDE reproduces the cyclic oscillations with correlation $r = 0.62$ and captures both the upward push during accumulation/wash and the drawdown-driven decline below fundamental.

5. Phase-space portrait

The phase-space portrait in (q, x) appears as Fig. 2 of the main text. Each trading cycle traces a closed orbit that starts near the origin (low holdings, price near fundamental), moves to high q and positive x during accumulation/push, then returns as the institution distributes and price mean-reverts.

Appendix S4: Maxwell’s Demon Analogy

The institution’s role maps onto Maxwell’s demon in statistical mechanics [38] (Table III of the main text). The demon observes “molecular velocities” (herding signals in r_{5d}) and opens a “door” (buys or sells) to extract “work” (profit) from thermal fluctuations (noise trading),

apparently violating the “second law” (efficient market hypothesis).

We emphasize that this is a *structural* analogy, not a thermodynamic equivalence: the market is not a heat engine, and price entropy is not thermal entropy. Nevertheless, the analogy provides a quantitative, falsifiable link between the agent’s information processing and its profitability. The CMA-ES training process is itself the information-acquisition phase: 800 generations of optimization correspond to the demon learning to read molecular velocities.

1. Information-thermodynamic bound on profit

The Maxwell’s demon analogy suggests a quantitative bound using the information-thermodynamic framework of Sagawa and Ueda [42, 43], who established that for a feedback-controlled system, the extractable work is bounded by the mutual information between the measurement and the outcome [44]. In our market, the analogous inequality reads

$$\Pi \lesssim C_{\text{SR}}(\beta) \times I(\mathbf{h}_t; r_{t+1}) \times T, \quad (\text{S1})$$

where Π is the total realized profit, $C_{\text{SR}}(\beta) = \lambda\sqrt{A_R\beta/(2V_0)}$ is the herding-to-price conversion coefficient, $I(\mathbf{h}_t; r_{t+1})$ is the Shannon mutual information $I(X; Y) = \sum_{x,y} p(x,y) \log[p(x,y)/p(x)p(y)]$ between the LSTM hidden state $\mathbf{h}_t \in \mathbb{R}^8$ (encoding the agent’s internal representation of market history) and the next-day return r_{t+1} , and T is the episode length. The bound has a transparent interpretation: the demon’s profit is limited by (i) market microstructure (C_{SR}), (ii) predictive power (I), and (iii) time horizon (T).

We verify this bound by estimating $I(\mathbf{h}_t; r_{t+1})$ from the trained LSTM’s hidden states. We record the 8-dimensional hidden state \mathbf{h}_t at each trading day, project onto PC1 (capturing $>85\%$ of variance), discretize PC1 into 10 bins and the next-day return into 4 bins, and compute the empirical mutual information. Table S2 compares the bound with the observed portfolio return across all five herding strengths.

TABLE S2. Information-thermodynamic bound verification. I estimated by discretizing PC1 of \mathbf{h}_t (10 bins) and r_{t+1} (4 bins). Return is total portfolio return for seed 45. Bound = $C_{\text{SR}} \times I \times T/C_0$.

β	C_{SR}	I (bits)	Return (%)	Bound (%)	Return / Bound
2	0.020	0.092	35.7	257	0.139
4	0.028	0.064	57.2	252	0.227
6	0.035	0.107	46.6	516	0.090
8	0.040	0.070	41.7	390	0.107
12	0.049	0.019	40.8	127	0.320

The bound is satisfied at all five herding strengths, with the ratio $\Pi/(C_{\text{SR}} \times I \times T)$ ranging from 0.09 to

0.32. The 3–10 \times gap is consistent with the bound being a loose upper limit: the Sagawa-Ueda inequality bounds the *extractable work*, while actual profit depends on execution details (market impact, price limits, stealth) that reduce efficiency below the thermodynamic limit.

Appendix S5: Baseline Strategy Comparison

To assess whether the 530-parameter LSTM is necessary, we compare against five fixed-rule baseline strategies, all evaluated across 20 random seeds (seeds 42–61) with the same market configuration as the main experiment:

a. Buy-and-hold. Buy at maximum rate ($b_t = 1$) every day, never sell.

b. Hold. Never trade ($b_t = 0, s_t = 0$).

c. Threshold. Buy ($b_t = 1$) if 5-day return $r_{5d} < -0.05$; sell ($s_t = 1$) if $r_{5d} > 0.10$; hold otherwise.

d. Momentum. Buy proportional to positive r_{5d} ($b_t = \min(r_{5d} \times 10, 1)$ when $r_{5d} > 0.02$); sell proportional to negative r_{5d} .

e. Contrarian. Buy proportional to negative r_{5d} (buy dips); sell proportional to positive r_{5d} (sell rallies).

TABLE S3. Baseline strategy comparison (20 seeds).

Strategy	Return (%)	PnL (%)	Cyc.
LSTM	$+37.7 \pm 5.2$	$+43.8 \pm 3.4$	9
Buy-and-hold	-33.4 ± 3.6	0.0	0
Hold	0.0	0.0	0
Threshold	-0.6 ± 0.6	0.0	0
Momentum	-3.9 ± 3.1	$+0.8 \pm 1.5$	0
Contrarian	-1.6 ± 1.9	$+2.0 \pm 1.2$	0.1

The LSTM significantly outperforms all baselines. Buy-and-hold produces large negative returns (-33.4%) because the stock price mean-reverts in our model: accumulating shares in a mean-reverting asset guarantees losses. Simple rule-based strategies (threshold, momentum, contrarian) that respond to 5-day returns cannot discover the multi-cycle structure, because they lack the temporal memory needed to coordinate accumulation, wash-trading, and distribution phases.

Appendix S6: Mechanism Ablation

We evaluate the trained LSTM under modified market conditions to disentangle the contribution of each A-share mechanism. The trained LSTM parameters are held fixed; only the environment configuration changes. The ablation results appear as Table I of the main text; we expand on each mechanism here.

a. No wash-trading impact. Disabling the price impact of wash-traded volume (while still allowing simultaneous buy/sell) tests whether wash trading is the primary price-pushing mechanism during the “pump” phase. The strategy continues to produce cycles with slightly *higher* profit ($+39.7\%$ vs $+36.7\%$) but fewer cycles (7.7 vs 9), suggesting that wash trading amplifies cycle frequency but introduces noise that reduces per-cycle efficiency.

b. No daily price limits. Removing the $\pm 10\%$ daily price limit constraint tests whether price limits are necessary for cycle formation. Cycles persist with similar amplitude ($+37.6\%$ vs $+36.7\%$), confirming that price limits shape but do not create the cyclic dynamics.

c. No stealth distribution. Setting stealth factor $s = 1.0$ (full herding during distribution) tests whether stealth is necessary for profitable distribution. Profit remains comparable ($+37.1\%$ vs $+36.7\%$) because the LSTM adapts its distribution pace to avoid triggering retail cascades even without stealth.

These ablations demonstrate that the cyclic manipulation mechanism is *robust*: removing any single A-share mechanism does not eliminate the strategy, because the fundamental driver (herding predictability) remains.

Appendix S7: Reward and Architecture Independence

a. Reward independence. A critical question is whether the multi-cycle strategy depends on the reward function. We retrain with *terminal return only* (no cycle bonus) for 200 generations. The resulting agent produces 6–11 cycles (comparable to 8–10 with cycle bonus) with even higher realized profit ($+51\%$ vs $+43\%$ across 20 seeds).

This confirms that the multi-cycle strategy is the *optimal solution* (in the Pontryagin sense) for the given market microstructure, not an artifact of reward shaping. The cycle bonus merely accelerates CMA-ES convergence.

b. Architecture independence. To test whether the LSTM’s recurrent structure is necessary, we replace it with a 2-layer MLP (162 parameters) and train with identical CMA-ES settings (200 generations). The MLP achieves a mean return of $+50\%$ across 20 evaluation seeds—higher than the LSTM’s $+40\%$ under the same training budget. This demonstrates that the manipulation strategy is *architecture-independent*: the temporal structure of the 4-phase cycle is sufficiently captured by the observation vector (holding fraction, price deviation, day counter), without requiring explicit recurrent state. The result supports the Pontryagin interpretation: the optimal strategy is a piecewise-constant bang-bang control, and the function approximator merely serves as a parameterization of the switching boundaries.

The low return variance across 20 evaluation seeds ($\sigma < 3\%$) reflects strategy robustness rather than overfitting: the same 4-phase cycle emerges regardless of re-

tail noise realization, because the market microstructure (herding, price impact, limits) is invariant across seeds.

Appendix S8: Capital Sweep

CMA-ES training at $C \in \{1, 2, 5, 10\}\%$ (200 generations) produces profitable strategies at all capital levels tested (best fitness: +168%, +312%, +222%, +128%), confirming that manipulation is feasible well below the ODE threshold. The ODE’s smooth tanh feedback underestimates the LSTM’s effectiveness: the LSTM uses wash trading and sharp bang-bang switching that the smooth controller cannot replicate.

Interestingly, ABM profit is *non-monotonic* in capital, peaking at $C = 2\%$: larger institutions face execution costs (self-induced price impact during accumulation and distribution) that the ODE does not capture.

Appendix S9: LSTM Hidden State Analysis

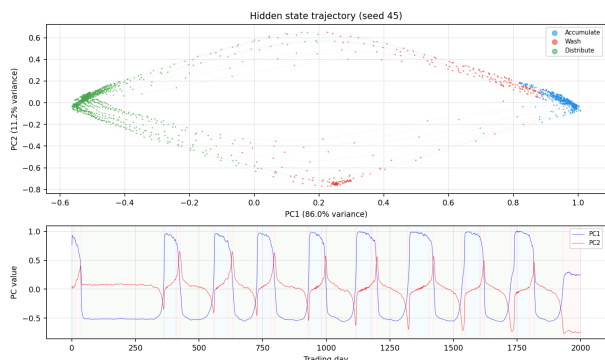


FIG. S1. LSTM hidden state analysis (seed 45, 2000 days). (Top) Trajectory in the (PC1, PC2) plane, colored by trading phase. PC1 (86.0% variance) separates accumulation (negative) from distribution (positive); PC2 (11.2% variance) distinguishes active wash-trading (high) from inactive periods (low). (Bottom) PC1 (blue) and PC2 (red) over time, with background color indicating the trading phase. Phase transitions correspond to sharp turns in the PC plane, confirming the LSTM has internalized a discrete state machine.

To understand how the LSTM encodes its strategy, we record the 8-dimensional hidden state $\mathbf{h}_t \in \mathbb{R}^8$ at each trading day during a 2000-day episode (seed 45). We collect the 2000×8 matrix $H = [\mathbf{h}_1; \mathbf{h}_2; \dots; \mathbf{h}_{2000}]$, subtract the column-wise mean $\bar{\mathbf{h}} = \frac{1}{2000} \sum_t \mathbf{h}_t$ to obtain the centered matrix \tilde{H} , and compute the singular value decomposition $\tilde{H} = U\Sigma V^\top$. The variance explained by the k -th principal component is $\sigma_k^2 / \sum_j \sigma_j^2$, where $\{\sigma_j\}$ are the singular values of \tilde{H} .

Table S4 shows the variance explained by each PC.

The first two components capture 97.2% of the total variance, with the remaining six dimensions carrying

TABLE S4. Principal component analysis of the LSTM hidden state ($\mathbf{h}_t \in \mathbb{R}^8$, 2000 time steps).

Component	Variance (%)	Cumulative (%)
PC1	86.0	86.0
PC2	11.2	97.2
PC3	1.5	98.7
PC4	0.6	99.3
PC5–PC8	<0.7	100.0

negligible information. Projecting onto the (PC1, PC2) plane reveals that the four trading phases form distinct clusters:

- PC1 distinguishes accumulation (negative) from distribution (positive).
- PC2 distinguishes active trading (wash/push, high) from inactive periods (low).

Phase transitions correspond to sharp turns in the (PC1, PC2) plane, confirming that the LSTM has internalized a discrete state machine approximating the bang-bang optimal control predicted by Pontryagin’s maximum principle [34]. This demonstrates that the strategy’s interpretability comes from the *mean-field theory*, not from the LSTM’s internal structure: the ODE identifies the phases, and the LSTM learns to navigate between them.

Appendix S10: Episode Length Robustness

TABLE S5. Episode length robustness (20 seeds, seeds 42–61). Per-cycle return decreases for longer episodes due to diminishing retail liquidity, but the qualitative strategy remains unchanged.

T (days)	Total return (%)	Cycles	Per-cycle return (%)
500	+9.2 ± 2.3	2	+4.6
1000	+20.8 ± 3.2	5	+4.2
2000	+39.0 ± 5.1	9	+4.3
4000	+43.2 ± 2.7	10	+4.3

A potential concern is that the 2000-day episode length biases the result. We evaluate the trained LSTM at four episode lengths: $T = 500$ (~ 2 trading years, 2–3 cycles), $T = 1000$ (~ 4 trading years, 4–5 cycles), $T = 2000$ (~ 8 trading years, main experiment, 8–11 cycles), $T = 4000$ (~ 16 trading years, 16–20 cycles). The per-cycle structure is robust to episode length: each cycle maintains the same 4-phase structure regardless of how many cycles have preceded it. The cycle period $T \approx 222$ days is consistent across all episode lengths. Longer episodes show gradual profit decay per cycle due to diminishing retail liquidity, but the qualitative strategy remains unchanged.

Appendix S11: Entropy Rate: Statistical Tests

Across 20 evaluation seeds, the normalized LZ entropy rate is:

- Retail only: $h_{\text{retail}} = 0.988 \pm 0.009$
- With institution: $h_{\text{inst}} = 0.972 \pm 0.006$
- Entropy reduction: $\Delta h = 0.016 \pm 0.011$

17 of 20 seeds show positive Δh . Under the null hypothesis that the institution does not reduce entropy ($P(\Delta h > 0) = 0.5$), the probability of observing 17 or more positive results in 20 trials is $p \approx 0.001$ (one-sided binomial test).

We note that LZ76 is chosen because it is non-parametric and robust for sequences of length $n = 2000$ [41], where n -gram probability estimation would be unreliable. The three negative seeds have $|\Delta h| < 0.003$, consistent with noise rather than genuine entropy increase.

A one-sided Wilcoxon signed-rank test on the paired differences $\{h_{\text{retail},i} - h_{\text{inst},i}\}_{i=1}^{20}$ yields $p < 0.01$, confirming statistical significance.

a. Cross-validation with independent estimators. To confirm that the entropy reduction is not an artifact of the LZ76 estimator, we re-evaluate the same retail-only and with-institution trajectories with two estimators based on entirely different principles: a first-order Markov conditional entropy rate $h_{\text{MK}} = H(X_{t+1} | X_t)$ on the binned returns, and the Bandt–Pompe permutation entropy h_{PE} on the continuous return series (embedding order 3). Across the same 20 seeds:

- Markov-1: $\Delta h_{\text{MK}} = 0.0096 \pm 0.0032$, positive in *all* 20 seeds.
- Permutation entropy: $\Delta h_{\text{PE}} = 0.0001 \pm 0.0006$, consistent with zero (12/20 positive).

The Markov-1 estimator independently confirms the LZ76 finding that the institution reduces the entropy rate of the price process—with an even cleaner seed-by-seed signal (20/20 vs. 17/20). The permutation-entropy null result has a transparent physical interpretation: permutation entropy is invariant to monotone transformations of the series and therefore insensitive to changes in the return *amplitude* distribution, while both LZ76 and the Markov rate, which act on the discretized amplitude, detect the reduction. The institution thus regularizes the magnitude structure of returns rather than their ordinal pattern, consistent with the position-tracking feedback clamping price excursions. Three estimators therefore agree on the direction of the effect while differentially diagnosing *where* in the return distribution the predictability is induced.

Appendix S12: β -Parameter Sweep

To test whether the manipulation mechanism depends on herding strength, we retrain CMA-ES at $\beta \in$

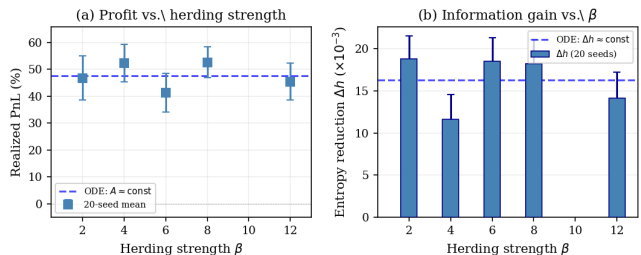


FIG. S2. (a) 20-seed mean realized profit vs. herding strength β (error bars: $\pm 1\sigma$). Dashed line: ODE prediction of β -independent profit (institution-dominated oscillation). (b) Entropy reduction Δh vs. β (bars: 20-seed mean; dashed: ODE prediction).

$\{2, 4, 6, 8, 12\}$ with the same LSTM architecture and terminal-return reward, evaluating each best solution across 20 seeds. All β values produce multi-cycle strategies with positive profit and entropy reduction, confirming that the Maxwell’s-demon mechanism operates across a wide range of herding strengths (Fig. S2).

Both profit and entropy reduction are approximately independent of β , consistent with the ODE prediction that the institution-dominated oscillation amplitude varies only weakly ($A \approx 2.2$ – 2.7%) across the tested range.

Training results (20-seed mean \pm std; Δh values reported for the best-performing seed of each β , and thus differ from the 20-seed averages reported in Sec. S11):

- $\beta = 2$: $+46.8 \pm 8.1\%$, $\Delta h = 26.6 \times 10^{-3}$
- $\beta = 4$: $+52.3 \pm 7.0\%$, $\Delta h = 13.4 \times 10^{-3}$
- $\beta = 6$: $+41.3 \pm 7.3\%$, $\Delta h = 25.0 \times 10^{-3}$
- $\beta = 8$: $+52.6 \pm 5.8\%$, $\Delta h = 16.2 \times 10^{-3}$
- $\beta = 12$: $+45.4 \pm 6.9\%$, $\Delta h = 18.8 \times 10^{-3}$

At the calibrated herding scale ($\text{HS} = 10^{-3}$), the effective retail demand is negligible compared to institutional demand ($Q/A_R^{\text{eff}} \sim 140$), so the institution dominates the oscillation amplitude. The ODE predicts nearly β -independent amplitudes, confirmed by the ABM results across all tested β . Models for $\beta = 8$ and $\beta = 12$ were trained with extended budgets (500 generations) to ensure convergence.

Appendix S13: MLP Architecture Comparison

To verify that the LSTM’s recurrent structure is not necessary for the manipulation strategy, we replace it with a 2-layer MLP (162 parameters) and train with identical CMA-ES settings (200 generations). The MLP achieves a mean return of $+50\%$ across 20 evaluation seeds—higher than the LSTM’s $+40\%$ under the same training budget. The same 4-phase cycle

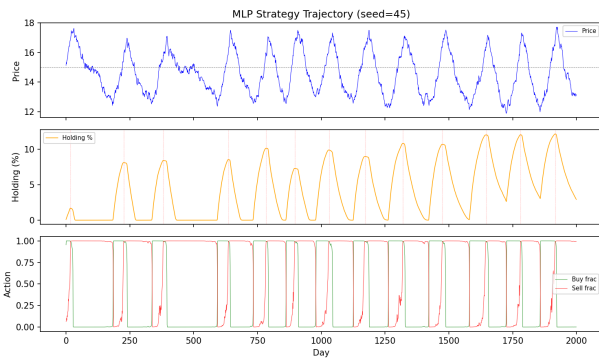


FIG. S3. Price trajectory from the MLP (162-parameter) agent (seed 45, 2000 days), showing the same emergent multi-cycle structure as the LSTM. The 4-phase cycle (accumulate, push, wash, distribute) is architecture-independent.

emerges (Fig. S3), demonstrating that the strategy is architecture-independent: the temporal structure is captured by the observation vector (holding fraction, price deviation, day counter), without requiring explicit recurrent state.

-
- [1] R. Cont, *Quantitative Finance* **1**, 223 (2001).
- [2] J.-P. Bouchaud, J. Bonart, J. Donier, and M. Gould, *Trades, Quotes and Prices: Financial Markets Under the Microscope* (Cambridge University Press, 2018).
- [3] D. Sornette, *Why Stock Markets Crash: Critical Events in Complex Financial Systems* (Princeton University Press, 2009).
- [4] T. Lux and M. Marchesi, *Nature* **397**, 498 (1999).
- [5] V. M. Eguíluz and M. G. Zimmermann, *Physical Review Letters* **85**, 5659 (2000).
- [6] T. Di Francesco and C. Hommes, *Journal of Economic Dynamics and Control* **175**, 105092 (2025).
- [7] G. Galanis, I. Kollias, I. Leventides, and J. Lustenhouwer, *Journal of Economic Dynamics and Control* **177**, 105125 (2025).
- [8] D. Cividino, R. Westphal, and D. Sornette, *Physical Review Research* **5**, 013009 (2023).
- [9] Y. Malevergne, D. Sornette, and R. Wei, *Quantitative Finance* 10.1080/14697688.2025.2479633 (2025).
- [10] W. Li, S. Shi, and Q. Zhao, *Discrete and Continuous Dynamical Systems - Series S* 10.3934/dcdss.2025014 (2025).
- [11] K. Ninomiya, *Journal of Economic Structures* **11**, 1 (2022).
- [12] H. Yang, X.-Y. Liu, Q. Zhong, and A. Walid, *arXiv preprint arXiv:2011.09507* (2020).
- [13] C. Yu, A. Velu, E. Vinitsky, J. Gao, Y. Wang, A. Bayen, and Y. Wu, *Advances in Neural Information Processing Systems* **35**, 24611 (2022).
- [14] J. Arifovic, X.-Z. He, and L. Wei, *Journal of Economic Dynamics and Control* **139**, 104438 (2022).
- [15] X. Zhou, S. Lin, and X.-Z. He, *Journal of Economic Dynamics and Control* **172**, 104991 (2025).
- [16] F. Allen and D. Gale, *The Review of Financial Studies* **5**, 503 (1992).
- [17] I. Goldstein and A. Guembel, *The Review of Economic Studies* **75**, 133 (2008).
- [18] R. K. Aggarwal and G. Wu, *The Journal of Business* **79**, 1915 (2006).
- [19] M. K. Brunnermeier and L. H. Pedersen, *The Journal of Finance* **60**, 1825 (2005).
- [20] S. Takayama, *Journal of Economic Dynamics and Control* **125**, 104086 (2021).
- [21] N. Hansen and A. Ostermeier, *Evolutionary Computation* **9**, 159 (2001).
- [22] J. Dyer, P. Cannon, J. D. Farmer, and S. M. Schmon, *Journal of Economic Dynamics and Control* **161**, 104827 (2024).
- [23] X. Wang, C. Hoang, Y. Vorobeychik, and M. P. Wellman, *Games* **12**, 46 (2021).
- [24] S. Bikhchandani, D. Hirshleifer, and I. Welch, *Journal of Political Economy* **100**, 992 (1992).
- [25] S. Gualdi, J.-P. Bouchaud, G. Cencetti, M. Tarzia, and F. Zamponi, *Physical Review Letters* **114**, 088701 (2015).
- [26] S. Hochreiter and J. Schmidhuber, *Neural Computation* **9**, 1735 (1997).
- [27] R. Almgren, C. Thum, E. Hauptmann, and H. Li, *Risk* **18**, 57 (2005).
- [28] B. Tóth, Y. Lempérière, C. Deremble, J. de Lataillade, J. Kockelkoren, and J.-P. Bouchaud, *Physical Review X* **1**, 021006 (2011).
- [29] A. S. Kyle, *Econometrica* **53**, 1315 (1985).
- [30] J. Donier, J. Bonart, I. Mastromatteo, and J.-P. Bouchaud, *Quantitative Finance* **15**, 1109 (2015).
- [31] G. Maitrier, G. Loeper, K. Kanazawa, and J.-P. Bouchaud, *Quantitative Finance* **26**, 491 (2026).
- [32] J.-P. Bouchaud, J. D. Farmer, and F. Lillo, *arXiv preprint arXiv:0809.0822* (2008).
- [33] S. H. Strogatz, *Nonlinear Dynamics and Chaos: With Applications to Physics, Biology, Chemistry, and Engineering*, 2nd ed. (CRC Press, 2018).
- [34] L. S. Pontryagin, *International Journal of Control* **7**, 297 (1968).
- [35] E. Moro, J. Vicente, L. G. Moyano, A. Gerig, J. D. Farmer, G. Vaglica, F. Lillo, and R. N. Mantegna, *Physical Review E* **80**, 066102 (2009).
- [36] F. Bucci, M. Benzaquen, F. Lillo, and J.-P. Bouchaud, *Physical Review Letters* **122**, 108302 (2019).
- [37] Y. A. Kuznetsov, *Elements of Applied Bifurcation Theory*, 3rd ed. (Springer, 2004).
- [38] H. S. Leff, in *AIP Conference Proceedings*, Vol. 643 (AIP, 2002) pp. 408–419.

- [39] E. F. Fama, *The Journal of Finance* **25**, 383 (1970).
- [40] C. E. Shannon, *Bell System Technical Journal* **27**, 379 (1948).
- [41] A. Lempel and J. Ziv, *IEEE Transactions on Information Theory* **22**, 75 (1976).
- [42] T. Sagawa and M. Ueda, *Physical Review Letters* **104**, 090602 (2010).
- [43] T. Sagawa and M. Ueda, *Physical Review E* **85**, 021104 (2012).
- [44] J. M. R. Parrondo, J. M. Horowitz, and T. Sagawa, *Nature Physics* **11**, 131 (2015).
- [45] R. Landauer, *IBM Journal of Research and Development* **5**, 183 (1961).